

# Climate change drove Late Miocene to Pliocene rise and fall of C<sub>4</sub> vegetation at the crossroads of Africa and Eurasia (Anatolia, Türkiye)

Maud J.M. Meijers<sup>1,2\*</sup>, Tamás Mikes<sup>2,3†</sup>, Bora Rojay<sup>4</sup>, H. Evren Çubukçu<sup>5</sup>, Erkan Aydar<sup>5,6</sup>, Tina Lüdecke<sup>2,7</sup>, Andreas Mulch<sup>2,8</sup>

5

<sup>1</sup>Department of Earth Sciences, NAWI Graz Geocenter, University of Graz, Heinrichstraße 26, 8010 Graz, Austria

<sup>2</sup>Senckenberg Biodiversity and Climate Research Centre, Senckenberganlage 25, 60325 Frankfurt am Main, Germany

<sup>3</sup>Independent geological consultant, Arnljot Gellines vei 35, 0657 Oslo, Norway

10 <sup>4</sup>Department of Geological Engineering, Middle East Technical University, 06800 Çankaya, Ankara, Türkiye

<sup>5</sup>Department of Geological Engineering, Hacettepe University, Beytepe Campus, 06800 Ankara, Türkiye

<sup>6</sup>Laboratoire Magmas et Volcans, CNRS, IRD, OPGC, Université Clermont Auvergne, F-63000 Clermont-Ferrand, France

<sup>7</sup>Emmy Noether Group for Hominin Meat Consumption, Max Planck Institute for Chemistry, Hahn-Meitner-Weg

15 1, 55128 Mainz, Germany

<sup>8</sup>Institute of Geosciences, Goethe University Frankfurt, Altenhöferallee 1, 60438 Frankfurt am Main, Germany

† Deceased

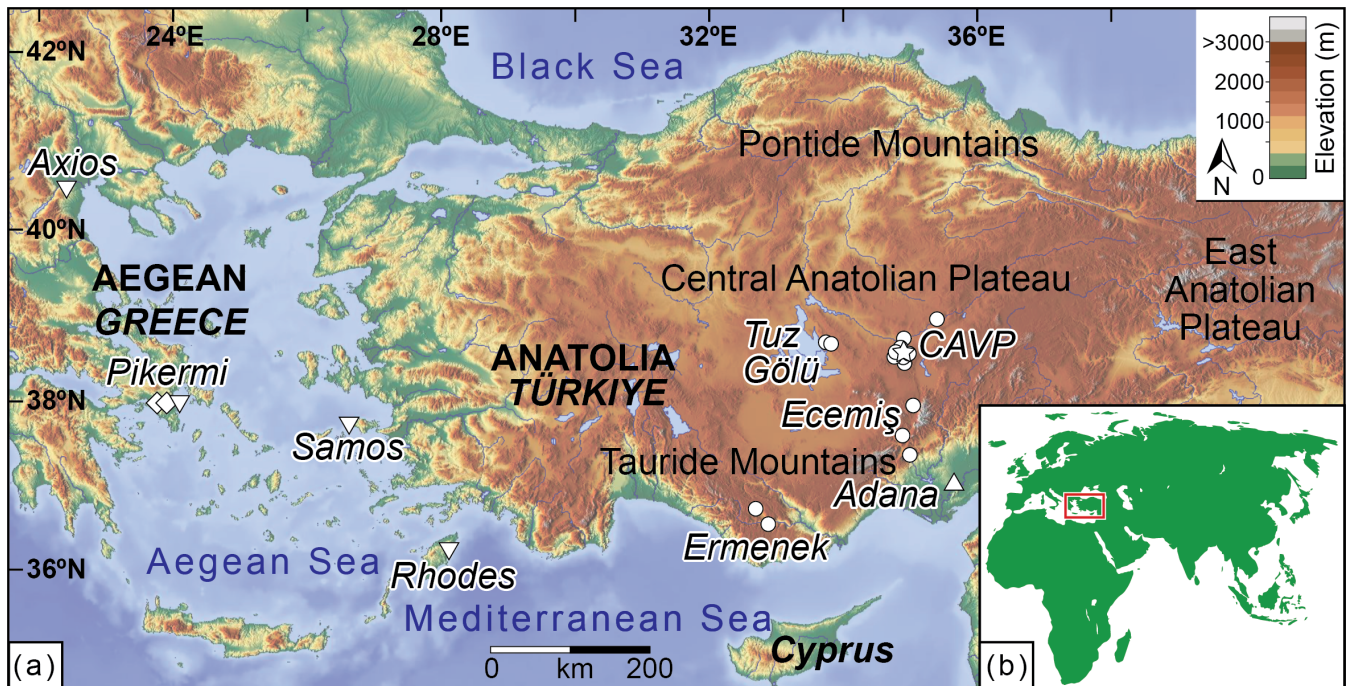
\*Correspondence to: Maud Meijers ([maud.meijers@uni-graz.at](mailto:maud.meijers@uni-graz.at))

20 **Abstract.** Life on Earth has been capitalizing on the C<sub>3</sub> photosynthetic pathway for 2.8 billion years. However, in the world's grasslands that emerged since the Paleogene, C<sub>4</sub> vegetation expanded dramatically between 8 and 3 Ma in response to climatic changes. Here we present the first comprehensive Late Miocene to Holocene  $\delta^{13}\text{C}$  soil carbonate record from the Eastern Mediterranean region (Anatolia) to reconstruct long-term geographic distributions of C<sub>3</sub> and C<sub>4</sub> plants, a region with patchy records compared to parts of Africa and Asia. Our results show a colonization of Anatolian floodplains by C<sub>4</sub> biomass by 9.9  
25 Ma, similar to regions in NW and E Africa, followed by a transition from this mixed C<sub>3</sub>-C<sub>4</sub> vegetation to C<sub>4</sub> dominance between ca. 7.1 Ma and 4.9 Ma. The transition to C<sub>4</sub> in Anatolia coincides with a similar shift from C<sub>3</sub> to C<sub>4</sub> vegetation in southern Asia and is generally attributed to the Late Miocene Cooling in response to decreasing atmospheric pCO<sub>2</sub>. However, the Anatolian paleoecosystem patterns are unique due to a rapid and permanent return to C<sub>3</sub> dominance in the Early Pliocene, which is not  
30 observed elsewhere and occurs simultaneously with the disappearance of the open environment-adapted large mammal  
Pikermian chronofauna. We propose that this return to C<sub>3</sub> vegetation was caused by paleoclimatic processes that regionally shifted precipitation from the warm to the cool season, resembling the modern Mediterranean climate. In conclusion, changes

in rainfall seasonality under subhumid climate, rather than increased aridity, drove the demise of C<sub>4</sub>-dominated floodplains and the open-environment adapted Pikermian chronofauna at the Eurasian-African crossroads.

## 35 1. Introduction

The earliest grassland ecosystems that emerged in the Paleogene were occupied by vegetation using the C<sub>3</sub> oxygenic photosynthetic pathway (Strömberg, 2011). However, many of the grassland environments that occupy ca. 40 % of Earth's landmass today are dominated by C<sub>4</sub> vegetation, including the Great Plains of North America, eastern South America, sub-Saharan Africa, southeast Asia, and northern Australia (Still et al., 2003). C<sub>4</sub> biomass consists of grasses (ca. 60 %), sedges, and dicots, and is adapted to conditions of drought, low atmospheric pCO<sub>2</sub>, and high temperatures (Sage, 2004). Although C<sub>4</sub> vegetation has been present since the Oligocene (Peppe et al., 2023; Urban et al., 2010), the rise to dominance of C<sub>4</sub> at the expense of C<sub>3</sub> vegetation in much of the world's grassland environments was delayed until the Late Miocene or even the Pliocene (Edwards et al., 2010; Strömberg, 2011).



45 **Figure 1:** (a) Topographic map of the studied Eastern Mediterranean region including sampling sites from this study and published studies in the Aegean (Greece) and Anatolia (Türkiye). Circles: this study; triangle Meijers et al. (2018); star: Lepetit (2010); diamonds: Böhme et al. (2017); inverted triangles: Quade et al. 1994). Geographic sampling areas correspond to those in Supplementary Table S1 and S3. CAVP= Central Anatolian Volcanic Province. (b) Location of the study area (red box) in (a) within the Old World.

50 Grassland expansion led to the evolution of open environment-adapted and hypsodont large herbivorous mammal communities of the Old World savannah paleobiome (OWSP) in Asia, East Africa, and southern Europe during the Late

Miocene (Kaya et al., 2018) until its Early Pliocene fragmentation (Böhme et al., 2021). The western Eurasian branch of the OSWP, the Pikermian chronofauna, reached its greatest geographic extent around ca. 8.0–6.6 Ma-ago and occupied large parts of Europe and Central Asia, including Anatolia (Eronen et al., 2009) when C<sub>4</sub> vegetation became dominant in certain grasslands of the Old World. Reconstructing the spread of C<sub>4</sub> vegetation through geologic time is crucial for identifying the global and regional climatic drivers behind faunal turnover, including the spread and decline of the Pikermian chronofauna. Direct evidence for the presence of C<sub>4</sub> vegetation in southern Europe and the Turkish-Iranian plateau region, however, is spatially and temporally patchy and incomplete (Böhme et al., 2017; Butiseacă et al., 2022; Urban et al., 2010).

Here, we reconstruct proportions of C<sub>4</sub> biomass in south-central Anatolia (Türkiye; Fig. 1), which is crucially located at the crossroads of well-studied regions in terms of vegetation dynamics in Africa and Asia (Behrensmeyer et al., 2007; Uno et al., 2011) and is presently characterized by a low amount of C<sub>4</sub> vegetation (< 10 %). We therefore analyze carbon isotopic compositions ( $\delta^{13}\text{C}$ ) of ca. 10 Ma to Holocene pedogenic carbonates from Anatolia. Based on the fundamentally different fractionation of carbon isotopes during photosynthesis of C<sub>3</sub> ( $\delta^{13}\text{C} = -26.7 \pm 12.3 \text{‰}$ ) and C<sub>4</sub> vegetation ( $\delta^{13}\text{C} = -12.5 \pm 1.1 \text{‰}$ ; Cerling et al., 1997) the transfer of this signal into materials such as pedogenic carbonates, mammalian tooth enamel, or leaf waxes can be used to reconstruct contributions of C<sub>4</sub> vegetation in deep time (Tippie and Pagani, 2007).

Our results of 447 pedogenic carbonate samples from sixteen sites show that C<sub>4</sub> plants spread to dominance in Anatolian floodplains during the Late Miocene and diminished to similar-to-modern proportions during the Pliocene. We compare the timing (Quade and Cerling, 1995) of floral overturn with the few available Anatolian (Türkiye) and Aegean (Greece) soil carbonate  $\delta^{13}\text{C}$  records, as well as with records of faunal overturn. We then assess the drivers of vegetation dynamics in terms of components of C<sub>4</sub> and C<sub>3</sub> vegetation in Anatolia and the Aegean by comparing their timing with other soil carbonate  $\delta^{13}\text{C}$  records from the Old World, as well as global marine climate records.

## 2. Material and methods

### 2.1 Pedogenic carbonate sampling

In Anatolia, eight pedogenic carbonate sites were sampled within the Central Anatolian Volcanic Province (CAVP) and two sites each adjacent to the Tuz Gölü and Ecemiş fault zones, as well as the Ermenek basin. Two additional sites were sampled within the Adana basin near the Mediterranean Sea (Fig. 1b, Table 1; see Supplementary Table S1 and Supplementary Text S1 for detailed site information). Site elevations from this study range between ca. 110 m and 1650 m a.s.l. and the sampled soil carbonates range in age from ca. 10 Ma to modern (Fig. 1b; Supplementary Table S1). Modern pedogenic carbonate samples consist of friable to weakly consolidated calcareous nodules typically 1 to 3 cm in diameter, from the B horizon of well-drained soils with a pink to red hackly appearance. Miocene to Pleistocene carbonate subsoil horizons developed within floodplain deposits. They comprise moderately consolidated to hard calcareous nodules ranging from 3 to 8 cm in diameter, or representative domains of dm-scale nodular carbonate layers. Whenever possible, pedogenic carbonate nodules and in some cases casts of taproots and fibrous roots, were collected from Bk horizons of cream to red-colored subsurface soils. Sampling choices were based on the availability of pedogenic carbonates in outcrops, which were taken over several months of fieldwork.

Where identifiable, pedogenic carbonate was sampled at a minimum soil depth of 30 cm to reduce the influence of atmospheric CO<sub>2</sub> (Cerling and Quade, 1993). Representative pictures of sampled outcrops and levels are shown in Supplementary Figure S1.

## 90 2.2 $\delta^{13}\text{C}$ of pedogenic carbonates

Powdered material from pedogenic carbonate samples was extracted with a diamond-tip dental drill. Only micritic parts devoid of clasts were drilled for analysis. A total of 447  $\delta^{13}\text{C}$  values were obtained for pedogenic carbonate samples from sixteen sites using a Thermo V mass spectrometer at the Institute of Geology (University of Hanover, Hanover, Germany) and a Thermo MAT 253 mass spectrometer at the joint Goethe University-Senckenberg BiK-F Stable Isotope Facility (Frankfurt, 95 Germany). Data were collected during multiple sessions in both labs.  $\delta^{18}\text{O}$  and  $\delta^{13}\text{C}$  values were evaluated simultaneously and are reported in Supplementary Table S1. The  $\delta^{18}\text{O}$  values that were obtained during the measurements were published in Meijers et al. (2025) and interpreted with respect to the surface uplift history of Anatolia. To assess intra- and inter-nodule variability, multiple measurements were performed on select single pedogenic carbonate nodules which were cross-sectioned from three sites: 10TG55 (n= 16, five nodules, three to four analyses per nodule), 10FD (n= 48, 25 nodules, of which three 100 nodules with six to 13 analyses per nodule), and 12C047–052 (n= 24, 16 nodules, of which two nodules with five measurements each; Supplementary Table S1). Powdered carbonate samples were digested in 100 % H<sub>3</sub>PO<sub>4</sub> and analyzed as CO<sub>2</sub> in continuous flow mode using above mentioned mass spectrometers interfaced with a Thermo GasBench II. Analytical procedures followed those of Spötl and Vennemann (2003), which includes corrections for scale, linearity, and drift. Raw isotopic ratios were calibrated against an in-house standard (Carrara marble;  $\delta^{13}\text{C}$ = 2.01 ‰ (V-PDB),  $\delta^{18}\text{O}$ = -1.74 ‰ (V-SMOW)), a synthetic Merck standard ( $\delta^{13}\text{C}$ = -35.69 ‰ (V-PDB),  $\delta^{18}\text{O}$ = 12.38 ‰ (V-SMOW)) and international carbonate reference material (NBS18). The in-house Carrara marble standard was weighed in for four different sample sizes for the linearity correction. Final isotopic ratios are reported against Vienna Pee Dee Belemnite (V-PDB), with analytical uncertainties that are typically better than 0.07 ‰. In the text, we refer to average  $\delta^{13}\text{C}$  values with 1 $\sigma$  standard deviations; averages, 1 $\sigma$ , and 2 $\sigma$  standard deviations, as well as medians, and 25<sup>th</sup> and 75<sup>th</sup> percentiles are displayed in Table 1 and Supplementary Table 115 S1. Pedogenic carbonate that formed in equilibrium with soil-respired CO<sub>2</sub> is enriched by ca. 14-17 ‰ in  $\delta^{13}\text{C}$  compared to CO<sub>2</sub> derived from root respiration and microbial decomposition of organic matter (e.g., Tipple and Pagani, 2007).

## 2.3 Pedogenic carbonate chronology

Age constraints for the paleosols containing the analyzed pedogenic carbonates from the CAP and the Tuz Gölü area are based 115 on radiometrically dated ignimbrite intercalations of the CAVP (Aydar et al., 2012; Özsayin et al., 2013). The stratigraphic framework for the sampled horizons is based on the ignimbrite stratigraphy and the published geochronological data (see Supplementary Text S1 and Supplementary Table S1). A composite section of the area of the southern CAVP where six sites were sampled shows the stratigraphic relationship between the sampled intervals (Supplementary Figure S1). The Quaternary

age for site 11AD is based on the 1:500,000 geological map of Adana (Ulu, 2002). Modern soil carbonate horizons were identified based on field relationships and assigned a Holocene age ( $5 \pm 5$  ka).

## 2.4 Reconstruction of climatic parameters

A reconstruction of paleobotany-derived climatic parameters of Anatolia (Fig. 2b, c) is based on the coexistence approach (Mosbrugger and Utescher, 1997). All data are listed in Supplementary Table S2.

## 2.5 Compilation of $\delta^{13}\text{C}$ values from Old World soil carbonates

The compilation of 12 Ma to Holocene soil carbonate  $\delta^{13}\text{C}$  values from Türkiye and Greece (Fig. 2a; Supplementary Table S3) includes data from Böhme et al. (2017), Lepetit (2010), and Quade et al. (1994). The compilation of 12 Ma to Holocene soil carbonate  $\delta^{13}\text{C}$  values from Asia and Africa (Fig. 3d, e) was retrieved from Fox et al. (2018). Datasets lacking age constraints were excluded. We also excluded elevated  $\delta^{13}\text{C}$  values from one multiproxy study on the Qaidam basin, which are attributed to low soil respiration rates in response to increased aridification (Zhuang et al., 2011). As such, the  $\delta^{13}\text{C}$  values may not be only interpreted in terms of variations in the dominating photosynthetic pathways (see also 4.1). Studies included in the Africa compilation (Fig. 3e): Aronson et al., (2008), Bestland and Krull (1999), Cerling and Hay (1986), Cerling et al. (1988, 1991, 2003, 2011), Kingston (1992), Levin et al. (2004, 2011), Plummer et al. (1999, 2009), Quade et al. (2004), Quinn et al. (2007), Sahnouni et al. (2011), Sikes (1994), Sikes et al. (1999), Sikes and Ashley (2007), WoldeGabriel et al. (2009), Wynn (2000, 2004), Wynn et al. (2006). Studies included in the Asia compilation (Fig. 3d): An et al. (2005), Behrensmeier et al. (2007), Ding and Yang (2000), Ghosh et al. (2004), Kaakinen et al. (2006), Passey et al. (2009), Quade et al. (1994), Quade and Cerling (1995), Sanyal et al. (2004), Yao et al. (2010).

## 3. Results

$\delta^{13}\text{C}$  values from the sixteen 10 Ma to Holocene sampled soil carbonate locations range from  $-9.5$  to  $3.4$  ‰, with an average of  $-5.4 \pm 3.4$  ‰ (Fig. 2a, Table 1, Supplementary Table S1). Based on their  $\delta^{13}\text{C}$  values (uncertainties reported at 1 sigma standard deviation ( $1\sigma$  SD)), we categorize the pedogenic carbonate record into four time intervals:

**9.9 Ma:**  $\delta^{13}\text{C}$  values of a single 9.9 Ma site ( $n=24$ ) in the Central Anatolian Volcanic Province (CAVP) average  $-5.2 \pm 2.6$  ‰.

**7.1 to 4.9 Ma:** The average  $\delta^{13}\text{C}$  value for the six sections ( $n=154$ ) from the CAVP is  $-1.2 \pm 2.0$  ‰, which is ca. 4 ‰ more positive than the 9.9 Ma dataset.

**3.9 Ma to 1.4 Ma:** Three pedogenic carbonates sites were sampled in the southern part of the CAP (CAVP and Tuz Gölü fault (TGF)), the Tauride Mountains (Ecemiş fault zone (EFZ) and Ermenek basin), and the Adana basin. The average  $\delta^{13}\text{C}$  value ( $n=188$ ) is  $-7.7 \pm 0.8$  ‰, which is nearly 7 ‰ more negative than the 7.1 to 4.9 Ma dataset.

**Holocene ( $5 \pm 5$  ka)**  $\delta^{13}\text{C}$  values from the six sections containing Holocene soil carbonates ( $n=87$ ) average  $-8.1 \pm 1.0$  ‰, which is within uncertainty identical to the 3.9 to 1.4 Ma datasets.

In summary, all soil carbonates younger than ca. 3.9 Ma yield nearly 7 ‰ lower  $\delta^{13}\text{C}$  values than the 7.1 to 4.9 Ma soil carbonates, as well as ca. 2.5 ‰ lower  $\delta^{13}\text{C}$  values than the ca. 9.9 Ma-old soil carbonate dataset (Fig. 2a).

155

**Table 1: Summary of pedogenic carbonate  $\delta^{13}\text{C}$  records from Anatolia (Türkiye, this study)**

Basin/area	Locality	Site/samples	Number of samples	Age (Ma)	$\Delta$ Age (Ma)
<b>Holocene (5 ± 5 ka)</b>					
Ermenek basin-Türkiye	Yalıncı	08Erm003A-004A**	2	0,005	0,005
Ermenek basin-Türkiye	Güneyyurt	08Erm006A-008A**	3	0,005	0,005
Tuz Gölü-Türkiye	Altınkaya	10TG55**	16	0,005	0,005
EFZ-Türkiye	Bulanlık	10BL01-07+09BL02-06**	12	0,005	0,005
EFZ-Türkiye	Fındıklı	10FD**	48	0,005	0,005
Adana basin-Türkiye	Gildirli	V01-128-136*	6	0,005	0,005
<b>Average : -8,1 ± 1,0 ‰ (n= 6; 1σ SD)</b>					
<b>Ca. 3.9 to 1.4 Ma</b>					
Adana basin-Türkiye	Baklalı and Misis	11AD01-95**	89	1,35	1,25
CAVP-Türkiye	Taşhan	14 MM 05-07**	3	3,81	1,08
Tuz Gölü-Türkiye	Cerit	10TG80, 87-91, 93-97**	96	3,86	0,20
<b>Average: -7,6 ± 0,5 ‰ (n= 3; 1σ SD)</b>					
<b>Ca. 7.1 Ma to 4.9 Ma</b>					
CAVP-Türkiye	Güzelöz	12C-070--084**	15	4,86	0,16
CAVP-Türkiye	Taşkınpaşa SW	12C-099--101**	3	5,68	0,66
CAVP-Türkiye	Şahinefendi	10CKK**	86	5,68	0,66
CAVP-Türkiye	Orta Tepe W	12C-002-023**	22	6,21	0,14
CAVP-Türkiye	Taşkınpaşa S	12C-063-069**	6	6,21	0,14
CAVP-Türkiye	Orta Tepe S	12C-025-046**	22	7,05	0,15
<b>Average: -0,9 ± 1,3 ‰ (n= 6; 1σ SD)</b>					
<b>Ca. 9.9 Ma</b>					
CAVP-Türkiye	Mustafapaşa	12C-047-062**	24	9,88	0,75

Latitude (°N)	Longitude (°E)	Average $\delta^{13}\text{C}$ (‰ V-PDB)	1 $\sigma$ SD (‰)	2 $\sigma$ SD (‰)	Median $\delta^{13}\text{C}$ (‰ V- PDB)	25th perc. (‰)	75th perc. (‰)
36,50844	32,95255	-9,0	0,4	0,9	-9,0	-9,2	-8,9
36,68815	32,76500	-8,8	0,7	1,4	-8,9	-9,2	-8,5
38,63093	33,80005	-8,5	0,1	0,2	-8,5	-8,5	-8,4
37,89825	35,10614	-6,3	0,6	1,2	-6,0	-6,8	-5,8
37,54615	34,94563	-8,4	0,4	0,8	-8,4	-8,7	-8,2
37,34890	35,05038	-7,4	2,1	4,3	-8,6	-8,7	-5,6
	***	-8,2	0,6	1,1	-8,3	-8,6	-7,9
38,90621	35,45562	-7,4	0,5	1,0	-7,3	-7,6	-7,1
38,61480	33,88557	-7,2	0,5	1,1	-7,0	-7,7	-6,8
38,39440	34,97231	1,0	2,1	4,3	1,1	0,3	2,6
38,48550	34,93776	0,1	1,1	2,3	-0,3	-0,6	0,5
38,46783	34,93887	-1,3	1,6	3,3	-1,3	-2,1	-0,4
38,47888	34,95045	-2,5	2,0	4,1	-2,6	-3,8	-1,1
38,48662	34,94468	-1,6	2,6	5,1	-0,6	-3,1	0,2
38,47325	34,95856	-1,1	2,1	4,1	-0,7	-2,6	0,8
38,57471	34,91145	-5,2	2,6	5,2	-6,0	-6,9	-3,9

160 SD= standard deviation; perc.= percentile; CAVP= Central Anatolian Volcanic Province; EFZ= Ecemis fault zone. For detailed geochronologies we refer to Supplementary Text S1. \* $\delta^{18}\text{O}$  values published in: Meijers et al. (2018); \*\* $\delta^{18}\text{O}$  values published in: Meijers et al. (2025); \*\*\*Locality 11AD consists of three sublocalities from time-equivalent deposits in a small area and were therefore merged. Baklali 1: 37,00761°N, 35,63193°E; Baklali 2: 37,01079°N, 35,63286°E; Baklali 3: 37,00203°N, 35,62834°E; Misis (Yakapinar): 36,97569°N, 35,62544°E. GPS coordinates in WGS84.

## 4. Discussion

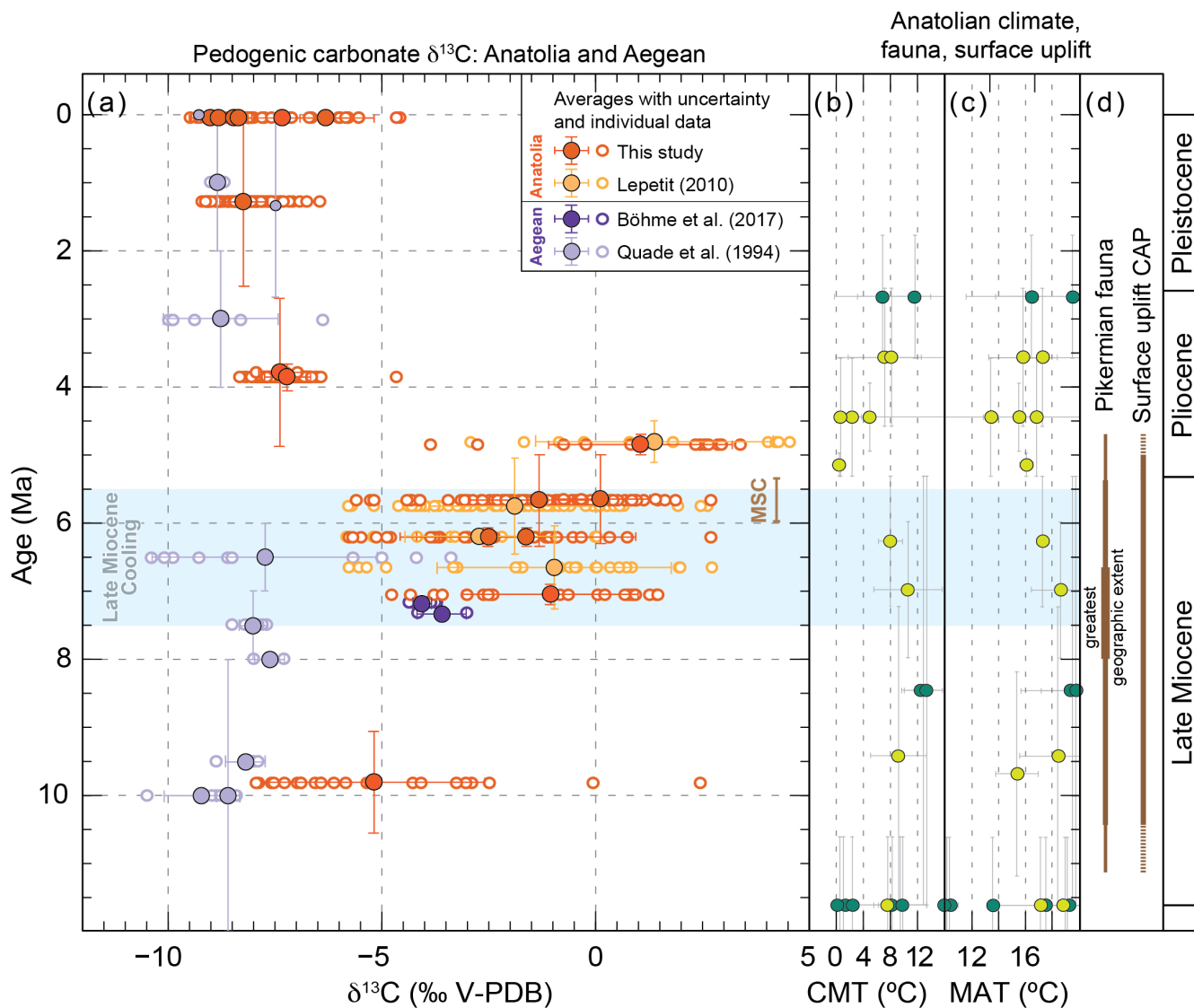
### 165 4.1 Soil carbonate $\delta^{13}\text{C}$ reveals variations of $\text{C}_3$ and $\text{C}_4$ vegetation in Anatolia and the Aegean

The 12 Ma to Holocene  $\delta^{13}\text{C}$  record from Anatolia shows large changes between the four time intervals (see Sect. 3 Results) and covers a wide range from  $-9.5\text{‰}$  to  $3.4\text{‰}$  (Fig. 2). This variation in  $\delta^{13}\text{C}$  values (up to  $12.9\text{‰}$ ) may reflect temporal changes in soil respiration rates, plant water stress, and/or the dominating photosynthetic pathway ( $\text{C}_3$  vs.  $\text{C}_4$ ) of biomass in Anatolia. We interpret obtained  $\delta^{13}\text{C}$  values (and associated  $\delta^{18}\text{O}$  values; Meijers et al., 2025) as primary (i.e. reflecting the isotopic ratios upon the formation of the carbonates), because the values are within a range typical of soil carbonates (e.g., Cerling and Quade, 1993). Additionally, the paleoaltimetry study by Meijers et al., (2025) that is based on the  $\delta^{18}\text{O}$  values associated with the  $\delta^{13}\text{C}$  values of this study includes two dual clumped isotope ( $\Delta_{47}$ ,  $\Delta_{48}$ ) temperatures. First, results for the ca. 5.4 Ma pedogenic carbonate sample (from CAVP site 10CKK, see also this study) and lake carbonate sample (from the Adana basin in southern Turkey) plot within error of the dual clumped isotope equilibrium line, which implies that their isotopic compositions are devoid of significant kinetic biases. Second, the obtained  $\Delta_{47}$  temperatures of  $15.6 \pm 3.3^\circ\text{C}$  (CAVP) and  $24.1 \pm 3.5^\circ\text{C}$  (Adana basin) show that the carbonates precipitated under conditions conformable with soil formation rather than with elevated diagenetic temperatures. More evidence for the primary origin of the sampled soil carbonates comes from the  $\delta^{18}\text{O}$  and  $\delta^{13}\text{C}$  values and thin sections of lake carbonate that was sampled in the same or similar fluvio-lacustrine host lithologies, which show no evidence of diagenetic alteration (Meijers et al., 2018; Meijers et al., 2020). Moreover, all sites within the Central Anatolian Plateau interior were buried only 170 m or less (Supplementary Table S1), except for Mustafapaşa (ca.  $9.9 \pm 0.8$  Ma; burial depth ca. 400 m). Low burial depths result from relatively low sedimentation rates (ca. 25–80 m/Myr; Supplementary Table S1) and rapid drainage integration and incision of the basins within maximal 2.5 Myrs after the latest deposition of the soil carbonate host lithologies (Brocard et al., 2021; Meijers et al., 2020).

Under conditions of low soil  $\text{CO}_2$  production, soil carbonates tend to form at shallower depths and may incorporate varying proportions of atmospheric  $\text{CO}_2$  (Cerling, 1984; Cerling and Quade, 1993), resulting in higher  $\delta^{13}\text{C}$  values (Caves et al., 2016; Licht et al., 2020). Particularly in dry ecosystems,  $\text{C}_3$  plants may yield increased  $\delta^{13}\text{C}$  values (Kohn, 2010). Although Anatolia is presently characterized by a climate with dry summers, all available paleobotanic datasets from the region suggest subhumid climatic conditions during the Late Miocene to Pliocene (Supplementary Table S2). We therefore interpret the variations in  $\delta^{13}\text{C}$  values of our 10 Ma to recent soil carbonate record to reflect significant changes in the relative contribution of  $\text{C}_3$  and  $\text{C}_4$  components of vegetation.

The large range of soil carbonate  $\delta^{13}\text{C}$  values of over  $10\text{‰}$  at ca. 9.9 Ma in Anatolia is consistent with a heterogeneous vegetation cover that includes both  $\text{C}_3$  and  $\text{C}_4$  plants, albeit with a dominance of  $\text{C}_3$  vegetation given an average  $\delta^{13}\text{C}$  of  $-5.2\text{‰}$ . Pedogenic carbonate  $\delta^{13}\text{C}$  values between 7.1 and 4.9 Ma, which average  $4.0\text{‰}$  more positive compared to  $\delta^{13}\text{C}$  values at 9.9 Ma indicate central Anatolian floodplain environments dominated by  $\text{C}_4$  vegetation (Fig. 2a). The dominance of  $\text{C}_4$  biomass between 7.1 and 4.9 Ma is consistent with published CAP  $\delta^{13}\text{C}$  values of pedogenic carbonate from this time interval (6.7 to 4.8 Ma; Fig. 2a; (Lepetit, 2010)), some of which were obtained from the same stratigraphic intervals. For the time intervals from 3.9 to 1.4 Ma and the Holocene our  $\delta^{13}\text{C}$  averages are significantly lower – by nearly  $7\text{‰}$  – than those from the 7.1 to

4.9 Ma interval, and by ca. 2.5 ‰ compared to the 9.9 Ma interval. This indicates the presence of floodplains dominated by C<sub>3</sub> vegetation after 3.9 Ma.



200

**Figure 2:** 12 to 0 Ma Anatolian and Aegean pedogenic carbonate  $\delta^{13}\text{C}$  records and Anatolian climatic, faunal, and surface uplift records. (a) Pedogenic carbonate  $\delta^{13}\text{C}$  values and their averages per site for this (orange) and published (purple, yellow) studies ((Böhme et al., 2017; Lepetit, 2010; Meijers et al., 2018; Quade et al., 1994) from Anatolia and the Aegean region. Small symbols with black stroke for sites with a single measurement. Global ‘Late Miocene Cooling’ (blue shading) according to Herbert et al. (2016). MSC: Messinian Salinity Crisis.

205

(b) and (c): Published paleobotanical data-based (Supplementary Table S2) cold month mean temperature (CMT) and mean annual temperature (MAT) reconstructions for Anatolia. Sites were subdivided in plateau interior and (near-)coastal because not only climate change but also surface uplift affected CMT and MAT on the plateau. Light green circles indicate sites that are currently within in the CAP interior

(ca. 1–1.5 km elevation), dark green circles indicate (near-)coastal sampling sites. (d) Periods during which the Pikermian chronofauna roamed Anatolia and surface uplift of the CAP occurred (onset: ca. 11 Ma; Meijers et al., 2018). The greatest geographic extent refers to the western Eurasian distribution of the Pikermian fauna (Eronen et al., 2009).

$\delta^{13}\text{C}$  values of ca. 9.3 to 5.3 Ma fossil equid tooth enamel (Rey et al., 2013), and ca. 10 to 6.5 Ma pedogenic carbonate  $\delta^{13}\text{C}$  records (Böhme et al., 2017; Quade et al., 1994; Supplementary Table S3) from the Aegean region (Greece) indicate  $\text{C}_3$  vegetation. However, phytoliths, as well as  $\delta^{13}\text{C}$  values of published pedogenic carbonate and fossil herbivore tooth enamel, imply the presence of  $\text{C}_4$  vegetation between ca. 9 Ma and 7 Ma in the CAVP (Kayseri-Özer et al., 2017; Lepetit, 2010), Pikermi and Samos (Aegean, Greece; Fig. 1b; Böhme et al., 2017; Quade et al., 1994), and Maragheh (Bernor et al., 2016; Biasatti et al., 2015; Strömberg et al., 2007). On Crete and Cyprus (Greece) ca. 5 ‰ variations in  $\delta^{13}\text{C}$  values of leaf waxes (long-chain n-alkanes produced by terrestrial plants), superimposed on an overall 4 ‰ increase in  $\delta^{13}\text{C}$  values between ca. 7 and 6 Ma, indicate the expansion of  $\text{C}_4$  vegetation (Butiseacă et al., 2022; Maysner et al., 2017) in response to Messinian climate cycles. Collectively, our data in combination with published datasets indicate that the geographic extent of  $\text{C}_4$  expansion in the Eastern Mediterranean region during the Late Miocene and earliest Pliocene may not have been restricted to Anatolia, but extended into the Aegean and the Iranian plateau. After 3.9 Ma (late Early Pliocene),  $\delta^{13}\text{C}$  values from Anatolian soil carbonates are similar to those derived from the Aegean (Fig. 1b; Quade et al., 1994) and indicate vegetation dominated by  $\text{C}_3$  biomass, which is the observed dominant vegetation type in Anatolia and the Aegean region today (< 10 %  $\text{C}_4$ ; Still et al., 2003).

#### 4.2 Late Miocene to Pliocene circum-Anatolian ecosystem reconstructions

Pedogenic carbonates from ca. 10 Ma to Holocene floodplain deposits in Anatolia indicate that the region has been characterized by rainfall seasonality since the Late Miocene, as their formation requires periodic soil drying (e.g., Zamanian et al., 2016). Furthermore, the dominance of  $\text{C}_4$  vegetation between 7.1 and 4.9 Ma in Anatolia, as reconstructed from our pedogenic carbonate  $\delta^{13}\text{C}$  values, suggests that open-habitat grasslands characterized portions of the landscape. This is supported by a) paleobotanical (macrofossils, pollen, and spores) data that suggest the introduction of steppe elements in Anatolia between 9 and 6 Ma (Denk et al., 2018), b) the (Middle-)Late Miocene rise of open-habitat grasslands in Anatolia and nearby Greece and Iran reconstructed from phytoliths (Strömberg et al., 2007), and c) the presence of the open-environment adapted Pikermian chronofauna in aforementioned regions (Eronen et al., 2009). However, macrofossil, pollen, and spore records from Anatolia, Greece, and Bulgaria (Denk et al., 2018) also sketch Late Miocene landscapes covered by evergreen needleleaf forests and mixed forests. As such, Denk et al. (2018) reject a cohesive savannah biome. We propose that the results from the paleobotanical and paleontological studies, as well as our stable isotope-based vegetation reconstructions, can be reconciled by heterogeneous Late Miocene Anatolian landscapes with largely interconnected forested as well as savannah-like environments (see also Fortelius et al., 2019).

The paleobotanical, paleontological, and soil carbonate records were all retrieved from ca. 11 to 4 Ma low-relief floodplains where fluvial and lacustrine deposits accumulated. Similar to today, the low-relief areas were interrupted by relict mountain ranges and local fault-controlled relief, but were not connected to marine basins. The fluvial and lacustrine records are currently accessible as a result of rapid latest Miocene to Pliocene drainage integration of the Anatolian plateau and subsequent river incision (Brocard et al., 2021; Meijers et al., 2020). As such, our soil carbonate  $\delta^{13}\text{C}$  records are biased towards partially preserved and incised intermontane floodplains and underrepresent vegetation dynamics of (potentially) forested and eroding topographic highs. Simultaneously, wind-blown pollen from forested montane areas are partially preserved in the fluvial and lacustrine records. Our  $\delta^{13}\text{C}$  soil carbonate record therefore highlights the importance of multi-proxy ecosystem reconstructions and solidifies evidence for a highly variable vegetation cover in Anatolia during the Late Miocene.

### 4.3 Timing and drivers of Late Miocene ecological change

Located at the crossroads of Africa, Asia, and Europe, the soil carbonate  $\delta^{13}\text{C}$  record of Anatolia bears the potential to identify paleoenvironmental dynamics specific to the spread of  $\text{C}_4$  vegetation in the Old World as well as to changing paleoclimatic conditions in the Mediterranean region. We compare the Anatolian soil carbonate  $\delta^{13}\text{C}$  record with available leaf wax, fossil tooth enamel, and soil carbonate  $\delta^{13}\text{C}$  records that constrain the initial expansion of  $\text{C}_4$  vegetation (Polissar et al., 2019) and its rise to dominance in the Old World grasslands during the Late Miocene (Fig. 3d-f). We conclude that the onset of  $\text{C}_4$  expansion in Anatolia during the Late Miocene (at the latest at ca. 9.9 Ma) is roughly coeval with the expansion of  $\text{C}_4$  ecosystems in NW and E Africa and predates its rise in other Asian and African regions (Fig. 3f). However,  $\text{C}_4$  vegetation dominated Anatolian floodplains and potentially parts of the Aegean by ca. 7.2 Ma, which roughly coincides with the start of the rapid rise to dominance of  $\text{C}_4$  vegetation in southern Asian grasslands between 7.8 and 7.2 Ma (Fig. 3c, d; e.g., Behrensmeier et al., 2007; Quade and Cerling, 1995; Tauxe and Feakins, 2020) and predates the rise to dominance of  $\text{C}_4$  vegetation in the grasslands of the southern East African Rift during the Pliocene (Fig. 3e; e.g., Cerling et al., 2011; Lüdecke et al., 2016).

The rise to dominance of  $\text{C}_4$  vegetation in East Asian grassland ecosystems is hypothesized to have occurred in response to declining atmospheric  $\text{pCO}_2$  levels that led to Late Miocene Cooling (LMC, ca. 7.5 to 5.5 Ma; Fig. 3b; Herbert et al., 2016) when low  $\text{pCO}_2$  provided an evolutionary advantage for  $\text{C}_4$  over  $\text{C}_3$  vegetation despite decreasing temperatures (e.g., Polissar et al., 2019; Wen et al., 2023). Worldwide, LMC is manifested in a sharp drop in sea surface temperatures (SSTs; Fig. 3b; (Herbert et al., 2016)) and its onset is accompanied by a sharp decrease in  $\delta^{13}\text{C}$  values of benthic foraminifera (Fig. 3a; Westerhold et al., 2020), which attests to a profound change in the global carbon cycle and consequently ocean circulation patterns (Holbourn et al., 2018). Climatic reconstructions from Anatolia based on the coexistence approach (Supplementary Table S2) indicate a ca. 2–3 °C decrease in mean annual and an up to 10 °C decrease in cold month mean temperatures during the Late Miocene in the CAP interior, although uncertainties in both reconstructed temperatures and ages are large (see Fig. 2b, c). Because the rise to dominance of  $\text{C}_4$  vegetation in Anatolian floodplains and possibly the Aegean occurred

275 simultaneously with its rise in southern Asian ecosystems and LMC (Fig. 3c, d) we suggest that it was caused by drivers that go beyond regional environmental changes such as surface uplift of the CAP since ca. 11 Ma (Fig. 2d; Meijers et al., 2018).

Whereas C<sub>4</sub> grassland expansion in southern Asia, the Chinese Loess Plateau, and Arabia coincided with aridification (Huang et al., 2007; Wen et al., 2023), the (gradual) expansion of C<sub>4</sub> vegetation in northern and eastern Africa was not driven by aridification (Crocker et al., 2022; Polissar et al., 2019). The latter also appears to hold for Anatolia and the Aegean, as  
280 indicated by Anatolian paleobotanical datasets suggesting subhumid conditions (e.g., Kayseri-Özer, 2017; Supplementary Table S3) and mesic environments in Anatolia and the Aegean instead (Denk et al., 2018).

Around ca. 8.0–6.6 Ma, the Pliocene chronofauna peaked in terms of geographic extent (Fig. 2d), including large parts of Europe and Central Asia (Eronen et al., 2009). We suggest that the spread of C<sub>4</sub> grasslands, which started before 9.9 Ma, and their dominance in floodplain environments by 7.2 Ma led to the expansion of the hypsodont Pliocene chronofauna  
285 in Anatolia. A similar process is observed in southern Asian grasslands, where combined soil and fossil mammal tooth enamel  $\delta^{13}\text{C}$  values show that long-term climate forcing changed the vegetation structure (C<sub>3</sub> to C<sub>4</sub>) between 8.5 and 6.0 Ma and led to the disappearance of most mammalian lineages that fed on C<sub>3</sub> vegetation (Badgley et al., 2008).

#### 4.4 Drivers and consequences of unique and persistent Early Pliocene C<sub>4</sub> decline

290 A marked decrease in our pedogenic carbonate  $\delta^{13}\text{C}$  values by approximately 7 ‰ from 4.9 to 3.9 Ma (Fig. 2a) implies a major overturn of Anatolian and potentially Aegean ecosystems. This transition led to the reemergence of landscapes dominated by C<sub>3</sub> vegetation, a feature that persists to the present day. Plant leaf wax  $\delta^{13}\text{C}$  values and pollen data from a sediment core in the Gulf of Aden reveal a brief reversal in the trend of increasing C<sub>4</sub> vegetation contributions between 4.9 and 4.6 Ma (Feakins et al., 2013). On and around the Chinese Loess Plateau, variations in C<sub>4</sub> and C<sub>3</sub> biomass have been linked to the strengthening  
295 and weakening of the East Asian summer monsoon (e.g., An et al., 2005; Passey et al., 2009; Yao et al., 2010). However, these fluctuations are not persistent over time. Therefore, the rapid and persistent Pliocene switch to C<sub>3</sub> vegetation is a feature that is so far unique to Anatolia. By contrast, southeast China (Fig. 3f) and regions in the New World (see e.g., Polissar et al., 2019) have been colonized by C<sub>4</sub> vegetation only after the return to C<sub>3</sub>-dominated vegetation in Anatolia. Given that the return to C<sub>3</sub> vegetation is geographically limited we assess potential causes for C<sub>4</sub> decline in Anatolia within a regional framework.

300 The Messinian Salinity Crisis (MSC) in the Mediterranean basin (5.96–5.33 Ma; e.g., Roveri et al., 2014) had the potential to alter the regional hydrologic cycle and hence vegetation. However, considering that the MSC is relatively short-lived and predates the decline of C<sub>4</sub> grasslands in Anatolia between 4.9 and 3.9 Ma, it is unlikely to be the main driver of the prolonged changes in the vegetation structure of the Eastern Mediterranean region.

During the Early Pliocene, regions adjacent to Anatolia also experienced significant environmental changes. In  
305 Central Europe, increased aridity led to the disappearance of open woodland, broad-leaf evergreen, and humid sclerophyllous taxa (Mosbrugger et al., 2005), some of which found refuge in Anatolia and the Eastern Mediterranean region (Eronen et al., 2009). Concurrently, Eastern Europe experienced a transition to cooler, drier conditions, leading to the expansion of grasslands and an enhanced fire regime since ca. 4.4 Ma (Feurdean and Vasiliev, 2019). The divergence in climate between a drier Central

Europe and a more humid Eastern Mediterranean region (Kovar-Eder, 2003) has been attributed to the deflection of the  
310 westerlies from Central Europe to the Mediterranean region (Eronen et al., 2009). Its timing coincides with strengthening of  
the Atlantic Meridional Overturning Circulation (AMOC) in response to shoaling of the Central American Seaway (CAS)  
around 4.8–4.0 Ma (e.g., Haug and Tiedemann, 1998). We therefore surmise that the increase in SSTs over the North Atlantic  
associated with AMOC strengthening (Karas et al., 2017) caused hydroclimatic changes over Europe and the Mediterranean  
region.

315

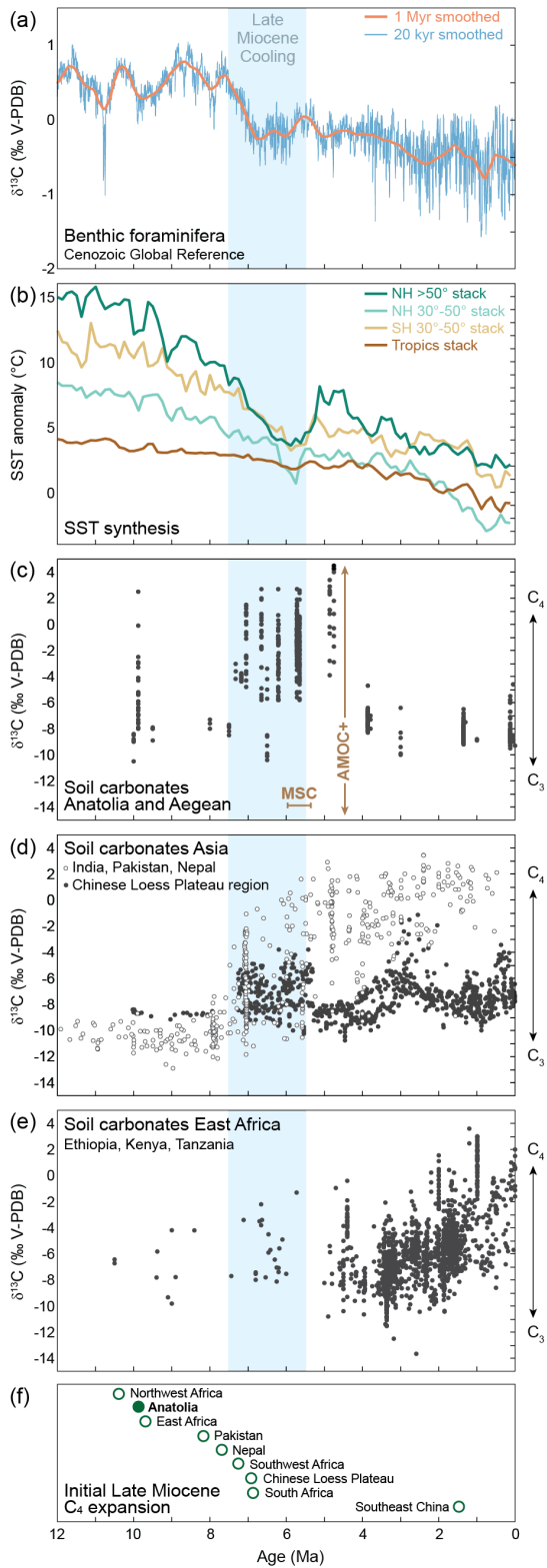


**Figure 3.** Climate and carbon isotope records spanning the last 12 Ma. (a) Cenozoic Global Reference (CENOGRID) benthic foraminifera  $\delta^{13}\text{C}$  curves, resampled and smoothed over 20 kyr (blue) and 1 Myr (red) periods (Westerhold et al., 2020). (b) SST anomalies for different hemispheric and latitude bins (Herbert et al., 2016). C–E: Compilation of soil carbonate  $\delta^{13}\text{C}$  values from Anatolia and the Aegean (c), Asia (d), and Africa (e). Asian and African datasets were retrieved from Fox et al. (2018). See Sect. 2.5. (f) Onset of the initial  $\text{C}_4$  expansion in the Old World from a compilation by Polissar et al. (2019) and including Anatolia (this study). Blue shading indicates time interval of Late Miocene Cooling (Herbert et al., 2016). NH= Northern Hemisphere, SH= Southern Hemisphere. MSC: Messinian Salinity Crisis (5.96 Ma–5.33 Ma; e.g. Roveri et al. (2014)), during which the restriction of the Mediterranean Basin led to drastic changes in local hydroclimate; AMOC+: strengthened Atlantic Meridional Overturning Circulation (AMOC) in response to shoaling of the Central American Seaway (ca. 4.8–4.0 Ma; Haug and Tiedemann, 1998) resulted in higher North Atlantic SSTs (Karas et al., 2017). We suggest that associated hydroclimatic changes over Europe and the Mediterranean region resulted in the decline of  $\text{C}_4$  vegetation in Anatolia (see Sect. 4.4).

Regions with prevalent  $\text{C}_4$  vegetation today are not only characterized by high growing season temperatures but also by warm season precipitation. In contrast, Anatolia presently experiences hot, dry Mediterranean summers and receives most of its precipitation from October through May (Schemmel et al., 2013; Türkeş and Erlat, 2005). Notably, leaf morphologies of Miocene species of evergreen oak (*Quercus* sect. *Ilex*) from southwest Türkiye and Aegean islands resemble modern Himalayan members, which suggests (summer-)humid climatic conditions (see Denk et al. (2018), but also Denk et al. (2014) and Velitzelos et al. (2014)). Additionally, Tortonian (ca. 11.6–7.2 Ma) paleoclimate simulations of Europe indicate humid to subhumid summer conditions in the northern Mediterranean region (Quan et al., 2014). We therefore propose that the shift from warm to cold season precipitation and the emergence of a Mediterranean-style climate drove the demise of  $\text{C}_4$  grasslands and a return to a  $\text{C}_3$ -dominated environment in Anatolia and the Aegean during the Early Pliocene (4.9 to 3.9 Ma). Such a change to more cold season precipitation has been shown to result in a strong and rapid (3–4 years) effect on the relative proportions of  $\text{C}_3$  and  $\text{C}_4$  vegetation during the 1930s Dust Bowl and was successfully reproduced in experimental studies in modern grasslands in the Great Plains (United States; Knapp et al., 2020).

The Early Pliocene demise of  $\text{C}_4$  biomass occurred simultaneously with significant large mammal faunal turnover (Huang et al., 2019) and the vanishing of open-landscape adapted large mammals from Anatolia (MN14; Eronen et al., 2009), which formed the last stronghold of the Pikermian chronofauna (Eronen et al., 2009). Our study therefore identifies long-term vegetation dynamics and indicates that Early Pliocene climate change profoundly and irreversibly transformed vegetation structures and drove a turnover in mammalian populations.

345

## 5. Conclusions

$\text{C}_4$  vegetation became ecologically dominant in Anatolian grasslands by 7.2 Ma, contemporaneous with similar developments in southern Asia and the Aegean. In contrast to the common association of  $\text{C}_4$  biomass expansion with arid conditions as the main driver, however,  $\text{C}_4$  expansion in Anatolia occurred under relatively humid conditions as indicated by consistent paleobotanical and stable isotope paleoclimate records. This suggests that a reduction in atmospheric  $\text{pCO}_2$  between ca. 7.5

350

and 5.5 Ma primarily drove C<sub>4</sub> expansion in this region. A distinctive, rapid decline of C<sub>4</sub> vegetation is observed in Anatolia between 4.9 and 3.9 Ma, leading to a C<sub>3</sub> vegetation-dominated environment that has persisted until today. We hypothesize that this shift, along with the disappearance of the Pikermian chronofauna, was influenced by the transition to a Mediterranean climate characterized by a change from warm to cold season precipitation.

355

**Data availability.** All supporting datasets are available as Supplementary information files that will be freely accessible upon publication.

**Author contributions:** MJM, TM, and AM: Conceptualization; MJM and TM: Investigation; MJM, TM, TL, AM: Methodology; MJM, TM, BR, HEÇ, EA, TL, and AM: Resources; MJM: Visualization; MJM: Writing – original draft; MJM, TM, BR, HEÇ, EA, TL, and AM: Writing – review & editing.

360

**Competing interests.** The authors declare that they have no conflict of interest.

### 365 **Acknowledgments**

We dedicate this publication to Tamás Mikes, who sadly passed away last year at a much too young age. We will remember Tamás as a joyful, curious, and exceptionally kind person and a knowledgeable and valued colleague. Without his dedication to field work and passion for science we would not have been able to conduct the presented research.

We express our sincere appreciation to the ESF TopoEurope VAMP and US-NSF CD-CAT research consortia for their significant contributions. AM acknowledges funding through ESF/DFG MU2845/1-1; EA and HEÇ acknowledge funding through Tübitak 107Y333. The authors acknowledge financial support by the University of Graz. We particularly thank A. Çiner (Hacettepe University, Ankara) for generous support throughout much of the study. Special thanks go to P. Ballato and F. Schemmel for field assistance. We thank E. Krsnik, U. Treffert (Senckenberg BiK-F), C. Wenske (Univ. Hannover), and J. Fiebig (Goethe University Frankfurt) for invaluable laboratory support. We thank Mine Sezgül Kayseri Özer, William Lukens, and an anonymous reviewer for their constructive comments and suggestions.

375

### **References**

An, Z., Huang, Y., Liu, W., Guo, Z., Clemens, S., Li, L., Prell, W., Ning, Y., Cai, Y., Zhou, W., Lin, B., Zhang, Q., Cao, Y., Qiang, X., Chang, H., and Wu, Z.: Multiple expansions of C<sub>4</sub> plant biomass in East Asia since 7 Ma coupled with strengthened monsoon circulation, *Geology*, 33, 705–708, <https://doi.org/10.1130/G21423.1>, 2005.

Aronson, J., Hailemichael, M., and Savin, S.: Hominid environments at Hadar from paleosol studies in a framework of Ethiopian climate change, *J Hum Evol*, 55, 532–550, <https://doi.org/10.1016/j.jhevol.2008.04.004>, 2008.

380

- Aydar, E., Schmitt, A. K., Çubukçu, H. E., Akin, L., Ersoy, O., Sen, E., Duncan, R. A., and Atici, G.: Correlation of ignimbrites in the central Anatolian volcanic province using zircon and plagioclase ages and zircon compositions, *Journal of Volcanology and Geothermal Research*, 213–214, 83–97, <https://doi.org/10.1016/j.jvolgeores.2011.11.005>, 2012.
- 385 Badgley, C., Barry, J. C., Le, M., Morgan, E., Nelson, S. V., Behrensmeyer, A. K., Cerling, T. E., and Pilbeam, D.: Ecological changes in Miocene mammalian record show impact of prolonged climatic forcing, 2008.
- Behrensmeyer, A. K., Quade, J., Cerling, T. E., Kappelman, J., Khan, I. A., Copeland, P., Roe, L., Hicks, J., Stubblefield, P., Willis, B. J., and Latorre, C.: The structure and rate of late Miocene expansion of C4 plants: Evidence from lateral variation in stable isotopes in paleosols of the Siwalik Group, northern Pakistan, *Bulletin of the Geological Society of America*, 119, 1486–1505, <https://doi.org/10.1130/B26064.1>, 2007.
- 390 Bernor, R. L., Mirzaie Atabadi, M., Meshida, K., and Wolf, D.: The Maragheh hipparions, late Miocene of Azarbaijan, Iran, *Paleobiodivers Paleoenviron*, 96, 453–488, <https://doi.org/10.1007/s12549-016-0235-2>, 2016.
- Bestland, E. A. and Krull, E. S.: Palaeoenvironments of Early Miocene Kisingiri volcano Proconsul sites: evidence from carbon isotopes, palaeosols and hydromagmatic deposits, *J Geol Soc London*, 156, 965–976, <https://doi.org/10.1144/gsjgs.156.5.0965>, 1999.
- 395 Biasatti, D., Bernor, R. L., and Cooper, L. W.: Insights on Late Miocene climate change and regional uplift in Maragheh Basin, eastern Azerbaijan Province, northwest Iran revealed by stable carbon and oxygen isotope analyses of fossil horse tooth enamel, in: 75th Annual Meeting, Society of Vertebrate Paleontology, 89–89, 2015.
- 400 Böhme, M., Spassov, N., Ebner, M., Geraads, D., Hristova, L., Kirscher, U., Kötter, S., Linnemann, U., Prieto, J., Roussiakis, S., Theodorou, G., Uhlig, G., and Winklhofer, M.: Messinian age & savannah environment of the possible hominin *Gracopithecus* from Europe, *PLoS One*, 12, <https://doi.org/10.1371/journal.pone.0177347>, 2017.
- Böhme, M., Spassov, N., Majidifard, M. R., Gärtner, A., Kirscher, U., Marks, M., Dietzel, C., Uhlig, G., El Atfy, H., Begun, D. R., and Winklhofer, M.: Neogene hyperaridity in Arabia drove the directions of mammalian dispersal between Africa and Eurasia, *Commun Earth Environ*, 2, 85, <https://doi.org/10.1038/s43247-021-00158-y>, 2021.
- 405 Brocard, G. Y., Meijers, M. J. M., Cosca, M. A., Salles, T., Willenbring, J., Teyssier, C., and Whitney, D. L.: Fast Pliocene integration of the Central Anatolian Plateau drainage: Evidence, processes, and driving forces, *Geosphere*, 17, 739–765, <https://doi.org/10.1130/GES02247.1>, 2021.
- Butiseacă, G. A., van der Meer, M. T. J., Kontakiotis, G., Agiadi, K., Thivaïou, D., Besiou, E., Antonarakou, A., Mulch, A., and Vasiliev, I.: Multiple crises preceded the Mediterranean Salinity Crisis: Aridification and vegetation changes revealed by biomarkers and stable isotopes, *Glob Planet Change*, 217, <https://doi.org/10.1016/j.gloplacha.2022.103951>, 2022.
- Caves, J. K., Moragne, D. Y., Ibarra, D. E., Bayshashov, B. U., Gao, Y., Jones, M. M., Zhamangara, A., Arzhannikova, A. V., Arzhannikov, S. G., and Chamberlain, C. P.: The Neogene de-greening of Central Asia, *Geology*, 44, 887–890, <https://doi.org/10.1130/G38267.1>, 2016.
- 415 Cerling, T. E.: The stable isotopic composition of modern soil carbonate and its relationship to climate, *Earth and Planetary Science Letters*, 229–240 pp., 1984.

- Cerling, T. E. and Hay, R. L.: An Isotopic Study of Paleosol Carbonates from Olduvai Gorge, *Quat Res*, 25, 63–78, [https://doi.org/10.1016/0033-5894\(86\)90044-X](https://doi.org/10.1016/0033-5894(86)90044-X), 1986.
- 420 Cerling, T. E. and Quade, J.: Stable Carbon and Oxygen Isotopes in Soil Carbonates, in: *Geophysical Monograph*, vol. 78, 217–231, <https://doi.org/10.1029/GM078p0217>, 1993.
- Cerling, T. E., Bowman, J. R., and O’Neil, J. R.: An isotopic study of a fluvial-lacustrine sequence: The Plio-Pleistocene koobi for sequence, East Africa, *Palaeogeogr Palaeoclimatol Palaeoecol*, 63, 335–356, [https://doi.org/10.1016/0031-0182\(88\)90104-6](https://doi.org/10.1016/0031-0182(88)90104-6), 1988.
- 425 Cerling, T. E., Quade, J., Ambrose, S. H., and Sikes, N. E.: Fossil soils, grasses, and carbon isotopes from Fort Ternan, Kenya: grassland or woodland?, *J Hum Evol*, 21, 295–306, [https://doi.org/10.1016/0047-2484\(91\)90110-H](https://doi.org/10.1016/0047-2484(91)90110-H), 1991.
- Cerling, T. E., Harris, J. M., MacFadden, B. J., Leakey, M. G., Quadek, J., Eisenmann, V., and Ehleringer, J. R.: Global vegetation change through the Miocene/Pliocene boundary, *Nature* © Macmillan Publishers Ltd, 1997.
- 430 Cerling, T. E., Harris, J. M., and Leakey, M. G.: 12.2. Isotope Paleoecology of the Nawata and Nachukui Formations at Lothagam, Turkana Basin, Kenya, in: *Lothagam*, Columbia University Press, 605–624, <https://doi.org/10.7312/leak11870-024>, 2003.
- Cerling, T. E., Wynn, J. G., Andanje, S. A., Bird, M. I., Korir, D. K., Levin, N. E., Mace, W., Macharia, A. N., Quade, J., and Remien, C. H.: Woody cover and hominin environments in the past 6 million years, *Nature*, 476, 51–56, <https://doi.org/10.1038/nature10306>, 2011.
- 435 Crocker, A. J., Naafs, B. D. A., Westerhold, T., James, R. H., Cooper, M. J., Röhl, U., Pancost, R. D., Xuan, C., Osborne, C. P., Beerling, D. J., and Wilson, P. A.: Astronomically controlled aridity in the Sahara since at least 11 million years ago, *Nat Geosci*, 15, 671–676, <https://doi.org/10.1038/s41561-022-00990-7>, 2022.
- Denk, T., Güner, T. H., and Grimm, G. W.: From mesic to arid: Leaf epidermal features suggest preadaptation in Miocene dragon trees (*Dracaena*), *Rev Palaeobot Palynol*, 200, 211–228, <https://doi.org/10.1016/j.revpalbo.2013.09.009>, 2014.
- 440 Denk, T., Zohner, C. M., Grimm, G. W., and Renner, S. S.: Plant fossils reveal major biomes occupied by the late Miocene Old-World Pliocene fauna, *Nat Ecol Evol*, 2, 1864–1870, <https://doi.org/10.1038/s41559-018-0695-z>, 2018.
- Ding, Z. L. and Yang, S. L.: C3/C4 vegetation evolution over the last 7.0 Myr in the Chinese Loess Plateau: evidence from pedogenic carbonate  $\delta^{13}C$ , *Palaeogeogr Palaeoclimatol Palaeoecol*, 160, 291–299, [https://doi.org/10.1016/S0031-0182\(00\)00076-6](https://doi.org/10.1016/S0031-0182(00)00076-6), 2000.
- 445 Edwards, E. J., Osborne, C. P., Strömberg, C. A. E., Smith, S. A., Bond, W. J., Christin, P. A., Cousins, A. B., Duvall, M. R., Fox, D. L., Freckleton, R. P., Ghannoum, O., Hartwell, J., Huang, Y., Janis, C. M., Keeley, J. E., Kellogg, E. A., Knapp, A. K., Leakey, A. D. B., Nelson, D. M., Saarela, J. M., Sage, R. F., Sala, O. E., Salamin, N., Still, C. J., and Tipple, B.: The origins of C4 Grasslands: Integrating evolutionary and ecosystem science, <https://doi.org/10.1126/science.1177216>, 30 April 2010.

- Eronen, J. T., Ataabadi, M. M., Micheels, A., Karne, A., Bernor, R. L., and Fortelius, M.: Distribution history and climatic controls of the Late Miocene Pikermian chronofauna, *Proc Natl Acad Sci U S A*, 106, 11867–11871, <https://doi.org/10.1073/pnas.0902598106>, 2009.
- Feakins, S. J., Levin, N. E., Liddy, H. M., Sieracki, A., Eglinton, T. I., and Bonnefille, R.: Northeast african vegetation change over 12 m.y, *Geology*, 41, 295–298, <https://doi.org/10.1130/G33845.1>, 2013.
- Feurdean, A. and Vasiliev, I.: The contribution of fire to the late Miocene spread of grasslands in eastern Eurasia (Black Sea region), *Sci Rep*, 9, <https://doi.org/10.1038/s41598-019-43094-w>, 2019.
- Fortelius, M., Bibi, F., Tang, H., Žliobaitė, I., Eronen, J. T., and Kaya, F.: The nature of the Old World savannah palaeobiome, <https://doi.org/10.1038/s41559-019-0857-7>, 1 April 2019.
- Fox, D. L., Pau, S., Taylor, L., Strömberg, C. A. E., Osborne, C. P., Bradshaw, C., Conn, S., Beerling, D. J., and Still, C. J.: Climatic Controls on C4 Grassland Distributions During the Neogene: A Model-Data Comparison, *Front Ecol Evol*, 6, <https://doi.org/10.3389/fevo.2018.00147>, 2018.
- Ghosh, P., Padia, J. T., and Mohindra, R.: Stable isotopic studies of palaeosol sediment from Upper Siwalik of Himachal Himalaya: Evidence for high monsoonal intensity during late Miocene?, *Palaeogeogr Palaeoclimatol Palaeoecol*, 206, 103–114, <https://doi.org/10.1016/j.palaeo.2004.01.014>, 2004.
- Haug, G. H. and Tiedemann, R.: Effect of the formation of the Isthmus of Panama on Atlantic Ocean thermohaline circulation, *Nature*, 393, 673–676, <https://doi.org/10.1038/31447>, 1998.
- Herbert, T. D., Lawrence, K. T., Tzanova, A., Peterson, L. C., Caballero-Gill, R., and Kelly, C. S.: Late Miocene global cooling and the rise of modern ecosystems, *Nat Geosci*, 9, 843–847, <https://doi.org/10.1038/ngeo2813>, 2016.
- Holbourn, A. E., Kuhnt, W., Clemens, S. C., Kochhann, K. G. D., Jöhnck, J., Lübbers, J., and Andersen, N.: Late Miocene climate cooling and intensification of southeast Asian winter monsoon, *Nat Commun*, 9, 1584, <https://doi.org/10.1038/s41467-018-03950-1>, 2018.
- Huang, S., Meijers, M. J. M., Eyres, A., Mulch, A., and Fritz, S. A.: Unravelling the history of biodiversity in mountain ranges through integrating geology and biogeography, *J Biogeogr*, 46, 1777–1791, <https://doi.org/10.1111/jbi.13622>, 2019.
- Huang, Y., Clemens, S. C., Liu, W., Wang, Y., and Prell, W. L.: Large-scale hydrological change drove the late Miocene C4 plant expansion in the Himalayan foreland and Arabian Peninsula, *Geology*, 35, 531, <https://doi.org/10.1130/G23666A.1>, 2007.
- Kaakinen, A., Sonninen, E., and Lunkka, J. P.: Stable isotope record in paleosol carbonates from the Chinese Loess Plateau: Implications for late Neogene paleoclimate and paleovegetation, *Palaeogeogr Palaeoclimatol Palaeoecol*, 237, 359–369, <https://doi.org/10.1016/j.palaeo.2005.12.011>, 2006.
- Karas, C., Nürnberg, D., Bahr, A., Groeneveld, J., Herrle, J. O., Tiedemann, R., and Demenocal, P. B.: Pliocene oceanic seaways and global climate, *Sci Rep*, 7, <https://doi.org/10.1038/srep39842>, 2017.
- Kaya, F., Bibi, F., Žliobaite, I., Eronen, J. T., Hui, T., and Fortelius, M.: The rise and fall of the Old World savannah fauna and the origins of the African savannah biome, *Nat Ecol Evol*, 2, 241–246, <https://doi.org/10.1038/s41559-017-0414-1>, 2018.

- Kayseri-Özer, M. S.: Cenozoic vegetation and climate change in Anatolia — A study based on the IPR-vegetation analysis, *Palaeogeogr Palaeoclimatol Palaeoecol*, 467, 37–68, <https://doi.org/10.1016/j.palaeo.2016.10.001>, 2017.
- 485 Kayseri-Özer, M. S., Karadenizli, L., Akgün, F., Oyal, N., Saraç, G., Şen, Ş., Tunoğlu, C., and Tuncer, A.: Palaeoclimatic and palaeoenvironmental interpretations of the Late Oligocene, Late Miocene–Early Pliocene in the Çankırı-Çorum Basin, *Palaeogeogr Palaeoclimatol Palaeoecol*, 467, 16–36, <https://doi.org/10.1016/j.palaeo.2016.05.022>, 2017.
- Kingston, J.: Stable isotopic evidence for hominid paleoenvironments in East Africa, PhD Thesis, Harvard University, 1–162 pp., 1992.
- 490 Knapp, A. K., Chen, A., Griffin-Nolan, R. J., Baur, L. E., Carroll, C. J. W., Gray, J. E., Hoffman, A. M., Li, X., Post, A. K., Slette, I. J., Collins, S. L., Luo, Y., and Smith, M. D.: Resolving the Dust Bowl paradox of grassland responses to extreme drought, *Proceedings of the National Academy of Sciences*, 117, 22249–22255, <https://doi.org/10.1073/pnas.1922030117>, 2020.
- Kohn, M. J.: Carbon isotope compositions of terrestrial C<sub>3</sub> plants as indicators of (paleo)ecology and (paleo)climate, *GEOLOGY ECOLOGY*, 107, 19691–19695, <https://doi.org/10.1073/pnas.1004933107/-/DCSupplemental>, 2010.
- 495 Kovar-Eder, J.: Vegetation dynamics in Europe during the Neogene, in: *Distribution and Migration of Tertiary Mammals in Eurasia. A volume in Honour of Hans de Bruijn.*, edited by: Reumer, J. W. F. and Wessels, W., DEINSEA, Rotterdam, 373–392, 2003.
- Lepetit, P.: Kohlenstoff-Isotopie miozäner Calcretes in Kappadokien (Türkei), PhD Thesis, Friedrich-Schiller-Universität  
500 Jena, Jena, 1–218 pp., 2010.
- Levin, N. E., Quade, J., Simpson, S. W., Semaw, S., and Rogers, M.: Isotopic evidence for Plio–Pleistocene environmental change at Gona, Ethiopia, *Earth Planet Sci Lett*, 219, 93–110, [https://doi.org/10.1016/S0012-821X\(03\)00707-6](https://doi.org/10.1016/S0012-821X(03)00707-6), 2004.
- Levin, N. E., Brown, F. H., Behrensmeyer, A. K., Bobe, R., and Cerling, T. E.: Paleosol carbonates from the Omo Group: Isotopic records of local and regional environmental change in East Africa, *Palaeogeogr Palaeoclimatol Palaeoecol*, 307, 75–  
505 89, <https://doi.org/10.1016/j.palaeo.2011.04.026>, 2011.
- Licht, A., Dupont-Nivet, G., Meijer, N., Caves Rugenstein, J., Schauer, A., Fiebig, J., Mulch, A., Hoorn, C., Barbolini, N., and Guo, Z.: Decline of soil respiration in northeastern Tibet through the transition into the Oligocene icehouse, *Palaeogeogr Palaeoclimatol Palaeoecol*, 560, <https://doi.org/10.1016/j.palaeo.2020.110016>, 2020.
- Lüdecke, T., Schrenk, F., Thiemeyer, H., Kullmer, O., Bromage, T. G., Sandrock, O., Fiebig, J., and Mulch, A.: Persistent C<sub>3</sub>  
510 vegetation accompanied Plio–Pleistocene hominin evolution in the Malawi Rift (Chiwondo Beds, Malawi), *J Hum Evol*, 90, 163–175, <https://doi.org/10.1016/j.jhevol.2015.10.014>, 2016.
- Maysner, J. P., Flecker, R., Marzocchi, A., Kouwenhoven, T. J., Lunt, D. J., and Pancost, R. D.: Precession driven changes in terrestrial organic matter input to the Eastern Mediterranean leading up to the Messinian Salinity Crisis, *Earth Planet Sci Lett*, 462, 199–211, <https://doi.org/10.1016/j.epsl.2017.01.029>, 2017.

- 515 Meijers, M. J. M., Brocard, G. Y., Cosca, M. A., Lüdecke, T., Teyssier, C., Whitney, D. L., and Mulch, A.: Rapid late Miocene surface uplift of the Central Anatolian Plateau margin, *Earth Planet Sci Lett*, 497, 29–41, <https://doi.org/10.1016/j.epsl.2018.05.040>, 2018.
- Meijers, M. J. M., Brocard, G. Y., Whitney, D. L., and Mulch, A.: Paleoenvironmental conditions and drainage evolution of the central Anatolian lake system (Turkey) during Late Miocene to Pliocene surface uplift, *Geosphere*, 16, 490–509,   
520 <https://doi.org/10.1130/GES02135.1>, 2020.
- Mosbrugger, V. and Utescher, T.: The coexistence approach — a method for quantitative reconstructions of Tertiary terrestrial palaeoclimate data using plant fossils, *Palaeogeogr Palaeoclimatol Palaeoecol*, 134, 61–86, [https://doi.org/10.1016/S0031-0182\(96\)00154-X](https://doi.org/10.1016/S0031-0182(96)00154-X), 1997.
- Mosbrugger, V., Utescher, T., and Dilcher, D. L.: Cenozoic continental climatic evolution of Central Europe, 2005.
- 525 Özsayın, E., Çiner, T. A., Rojay, F. B., Dirik, R. K., Melnick, D., Fernandez-Blanco, D., Bertotti, G., Schildgen, T. F., Garcin, Y., Strecker, M. R., and Sudo, M.: Plio-Quaternary extensional tectonics of the Central Anatolian Plateau: a case study from the Tuz Gölü Basin, Turkey, *Turkish Journal of Earth Sciences*, <https://doi.org/10.3906/yer-1210-5>, 2013.
- Passey, B. H., Ayliffe, L. K., Kaakinen, A., Zhang, Z., Eronen, J. T., Zhu, Y., Zhou, L., Cerling, T. E., and Fortelius, M.: Strengthened East Asian summer monsoons during a period of high-latitude warmth? Isotopic evidence from Mio-Pliocene   
530 fossil mammals and soil carbonates from northern China, *Earth Planet Sci Lett*, 277, 443–452, <https://doi.org/10.1016/j.epsl.2008.11.008>, 2009.
- Peppe, D. J., Cote, S. M., Deino, A. L., Fox, D. L., Kingston, J. D., Kinyanjui, R. N., Lukens, W. E., MacLachy, L. M., Novello, A., Strömberg, C. A. E., Driese, S. G., Garrett, N. D., Hillis, K. R., Jacobs, B. F., Jenkins, K. E. H., Kityo, R. M., Lehmann, T., Manthi, F. K., Mbua, E. N., Michel, L. A., Miller, E. R., Mugume, A. A. T., Muteti, S. N., Nengo, I. O., Oginga,   
535 K. O., Phelps, S. R., Polissar, P., Rossie, J. B., Stevens, N. J., Uno, K. T., and McNulty, K. P.: Oldest evidence of abundant C4 grasses and habitat heterogeneity in eastern Africa, *Science* (1979), 380, 173–177, <https://doi.org/10.1126/science.abq2834>, 2023.
- Plummer, T., Bishop, L. C., Ditchfield, P., and Hicks, J.: Research on Late Pliocene Oldowan Sites at Kanjera South, Kenya, *J Hum Evol*, 36, 151–170, <https://doi.org/10.1006/jhev.1998.0256>, 1999.
- 540 Plummer, T. W., Ditchfield, P. W., Bishop, L. C., Kingston, J. D., Ferraro, J. V., Braun, D. R., Hertel, F., and Potts, R.: Oldest Evidence of Toolmaking Hominins in a Grassland-Dominated Ecosystem, *PLoS One*, 4, e7199, <https://doi.org/10.1371/journal.pone.0007199>, 2009.
- Polissar, P. J., Rose, C., Uno, K. T., Phelps, S. R., and deMenocal, P.: Synchronous rise of African C4 ecosystems 10 million years ago in the absence of aridification, *Nat Geosci*, 12, 657–660, <https://doi.org/10.1038/s41561-019-0399-2>, 2019.
- 545 Quade, J. and Cerling, T. E.: Expansion of C4 grasses in the Late Miocene of Northern Pakistan: evidence from stable isotopes in paleosols, *Palaeogeogr Palaeoclimatol Palaeoecol*, 115, 91–116, [https://doi.org/10.1016/0031-0182\(94\)00108-K](https://doi.org/10.1016/0031-0182(94)00108-K), 1995.

- Quade, J., Solounias, N., and Cerling, T. E.: Stable isotopic evidence from paleosol carbonates and fossil teeth in Greece for forest or woodlands over the past 11 Ma, *Palaeogeogr Palaeoclimatol Palaeoecol*, 108, 41–53, [https://doi.org/10.1016/0031-0182\(94\)90021-3](https://doi.org/10.1016/0031-0182(94)90021-3), 1994.
- 550 Quade, J., Levin, N., Semaw, S., Stout, D., Renne, P., Rogers, M., and Simpson, S.: Paleoenvironments of the earliest stone toolmakers, Gona, Ethiopia, *Geol Soc Am Bull*, 116, 1529–1544, <https://doi.org/10.1130/B25358.1>, 2004.
- Quan, C., Liu, Y. S. C., Tang, H., and Utescher, T.: Miocene shift of European atmospheric circulation from trade wind to westerlies, *Sci Rep*, 4, <https://doi.org/10.1038/srep05660>, 2014.
- Quinn, R. L., Lepre, C. J., Wright, J. D., and Feibel, C. S.: Paleogeographic variations of pedogenic carbonate  $\delta^{13}\text{C}$  values  
555 from Koobi Fora, Kenya: implications for floral compositions of Plio-Pleistocene hominin environments, *J Hum Evol*, 53, 560–573, <https://doi.org/10.1016/j.jhevol.2007.01.013>, 2007.
- Rey, K., Amiot, R., Lécuyer, C., Koufos, G. D., Martineau, F., Fourel, F., Kostopoulos, D. S., and Merceron, G.: Late Miocene climatic and environmental variations in northern Greece inferred from stable isotope compositions ( $\delta^{18}\text{O}$ ,  $\delta^{13}\text{C}$ ) of equid teeth apatite, *Palaeogeogr Palaeoclimatol Palaeoecol*, 388, 48–57, <https://doi.org/10.1016/j.palaeo.2013.07.021>, 2013.
- 560 Roveri, M., Flecker, R., Krijgsman, W., Lofi, J., Lugli, S., Manzi, V., Sierro, F. J., Bertini, A., Camerlenghi, A., De Lange, G., Govers, R., Hilgen, F. J., Hübscher, C., Meijer, P. T., and Stoica, M.: The Messinian Salinity Crisis: Past and future of a great challenge for marine sciences, *Mar Geol*, 352, 25–58, <https://doi.org/10.1016/j.margeo.2014.02.002>, 2014.
- Sage, R. F.: The evolution of C<sub>4</sub> photosynthesis, *New Phytologist*, 161, 341–370, <https://doi.org/10.1046/j.1469-8137.2004.00974.x>, 2004.
- 565 Sahnouni, M., Van der Made, J., and Everett, M.: Ecological background to Plio-Pleistocene hominin occupation in North Africa: the vertebrate faunas from Ain Boucherit, Ain Hanech and El-Kherba, and paleosol stable-carbon-isotope studies from El-Kherba, Algeria, *Quat Sci Rev*, 30, 1303–1317, <https://doi.org/10.1016/j.quascirev.2010.01.002>, 2011.
- Sanyal, P., Bhattacharya, S. K., Kumar, R., Ghosh, S. K., and Sangode, S. J.: Mio-Pliocene monsoonal record from Himalayan foreland basin (Indian Siwalik) and its relation to vegetational change, *Palaeogeogr Palaeoclimatol Palaeoecol*, 205, 23–41,  
570 <https://doi.org/10.1016/j.palaeo.2003.11.013>, 2004.
- Schemmel, F., Mikes, T., Rojay, B., and Mulch, A.: The impact of topography on isotopes in precipitation across the central Anatolian plateau (Turkey), *Am J Sci*, 313, 61–80, <https://doi.org/10.2475/02.2013.01>, 2013.
- Sikes, N. E.: Early hominid habitat preferences in East Africa: Paleosol carbon isotopic evidence, *J Hum Evol*, 27, 25–45, <https://doi.org/10.1006/jhev.1994.1034>, 1994.
- 575 Sikes, N. E. and Ashley, G. M.: Stable isotopes of pedogenic carbonates as indicators of paleoecology in the Plio-Pleistocene (upper Bed I), western margin of the Olduvai Basin, Tanzania, *J Hum Evol*, 53, 574–594, <https://doi.org/10.1016/j.jhevol.2006.12.008>, 2007.
- Sikes, N. E., Potts, R., and Behrensmeier, A. K.: Early Pleistocene habitat in Member 1 Ologesailie based on paleosol stable isotopes, *J Hum Evol*, 37, 721–746, <https://doi.org/10.1006/jhev.1999.0343>, 1999.

- 580 Spötl, C. and Vennemann, T. W.: Continuous-flow isotope ratio mass spectrometric analysis of carbonate minerals, *Rapid Communications in Mass Spectrometry*, 17, 1004–1006, <https://doi.org/10.1002/rcm.1010>, 2003.
- Still, C. J., Berry, J. A., Collatz, G. J., and DeFries, R. S.: Global distribution of C<sub>3</sub> and C<sub>4</sub> vegetation: Carbon cycle implications, *Global Biogeochem Cycles*, 17, <https://doi.org/10.1029/2001gb001807>, 2003.
- Strömberg, C. A. E.: Evolution of grasses and grassland ecosystems, *Annu Rev Earth Planet Sci*, 39, 517–544, 585 <https://doi.org/10.1146/annurev-earth-040809-152402>, 2011.
- Strömberg, C. A. E., Werdelin, L., Friis, E. M., and Saraç, G.: The spread of grass-dominated habitats in Turkey and surrounding areas during the Cenozoic: Phytolith evidence, *Palaeogeogr Palaeoclimatol Palaeoecol*, 250, 18–49, <https://doi.org/10.1016/j.palaeo.2007.02.012>, 2007.
- Tauxe, L. and Feakins, S.J.: A Reassessment of the Chronostratigraphy of Late Miocene C<sub>3</sub>–C<sub>4</sub> Transitions, *Palaeogeogr* 590 *Palaeoclimatol*, 35, <https://doi.org/10.1029/2020PA003857>, 2020.
- Tipple, B. J. and Pagani, M.: The early origins of terrestrial C<sub>4</sub> photosynthesis, *Annu Rev Earth Planet Sci*, 35, 435–461, <https://doi.org/10.1146/annurev.earth.35.031306.140150>, 2007.
- Türkeş, M. and Erlat, E.: Climatological responses of winter precipitation in Turkey to variability of the North Atlantic Oscillation during the period 1930–2001, *Theor Appl Climatol*, 81, 45–69, <https://doi.org/10.1007/s00704-004-0084-1>, 2005.
- 595 Ulu, Ü.: 1:500.000 Geological Map of Turkey, Adana, 2002.
- Uno, K. T., Cerling, T. E., Harris, J. M., Kunitatsu, Y., Leakey, M. G., Nakatsukasa, M., and Nakaya, H.: Late Miocene to Pliocene carbon isotope record of differential diet change among East African herbivores, *Proc Natl Acad Sci U S A*, 108, 6509–6514, <https://doi.org/10.1073/pnas.1018435108>, 2011.
- Urban, M. A., Nelson, D. M., Jimenez-Moreno, G., Chateaufneuf, J.-J., Pearson, A., and Hu, F. S.: Isotopic evidence of C<sub>4</sub> 600 grasses in southwestern Europe during the Early Oligocene–Middle Miocene, *Geology*, 38, 1091–1094, <https://doi.org/10.1130/G31117.1>, 2010.
- Velitzelos, D., Bouchal, J. M., and Denk, T.: Review of the Cenozoic floras and vegetation of Greece, <https://doi.org/10.1016/j.revpalbo.2014.02.006>, 2014.
- Wen, Y., Zhang, L., Holbourn, A. E., Zhu, C., Huntington, K. W., Jin, T., Li, Y., and Wang, C.: CO<sub>2</sub>-forced Late Miocene 605 cooling and ecosystem reorganizations in East Asia, *Proc Natl Acad Sci U S A*, 120, <https://doi.org/10.1073/pnas.2214655120>, 2023.
- Westerhold, T., Marwan, N., Drury, A. J., Liebrand, D., Agnini, C., Anagnostou, E., Barnet, J. S. K., Bohaty, S. M., De Vleeschouwer, D., Florindo, F., Frederichs, T., Hodell, D. A., Holbourn, A. E., Kroon, D., Laurentano, V., Littler, K., Lourens, L. J., Lyle, M., Pälike, H., Röhl, U., Tian, J., Wilkens, R. H., Wilson, P. A., and Zachos, J. C.: An astronomically dated record 610 of Earth’s climate and its predictability over the last 66 million years, *Science* (1979), 369, 1383–1387, <https://doi.org/10.1126/science.aba6853>, 2020.
- WoldeGabriel, G., Ambrose, S. H., Barboni, D., Bonnefille, R., Bremond, L., Currie, B., DeGusta, D., Hart, W. K., Murray, A. M., Renne, P. R., Jolly-Saad, M. C., Stewart, K. M., and White, T. D.: The Geological, Isotopic, Botanical, Invertebrate,

- and Lower Vertebrate Surroundings of *Ardipithecus ramidus*, *Science* (1979), 326, 65,  
615 <https://doi.org/10.1126/science.1175817>, 2009.
- Wynn, J. G.: Paleosols, stable carbon isotopes, and paleoenvironmental interpretation of Kanapoi, Northern Kenya, *J Hum Evol*, 39, 411–432, <https://doi.org/10.1006/jhev.2000.0431>, 2000.
- Wynn, J. G.: Influence of Plio-Pleistocene aridification on human evolution: Evidence from paleosols of the Turkana Basin, Kenya, *Am J Phys Anthropol*, 123, 106–118, <https://doi.org/10.1002/ajpa.10317>, 2004.
- 620 Wynn, J. G., Alemseged, Z., Bobe, R., Geraads, D., Reed, D., and Roman, D. C.: Geological and palaeontological context of a Pliocene juvenile hominin at Dikika, Ethiopia, *Nature*, 443, 332–336, <https://doi.org/10.1038/nature05048>, 2006.
- Yao, Z., Xiao, G., Wu, H., Liu, W., and Chen, Y.: Plio-Pleistocene vegetation changes in the North China Plain: Magnetostratigraphy, oxygen and carbon isotopic composition of pedogenic carbonates, *Palaeogeogr Palaeoclimatol Palaeoecol*, 297, 502–510, <https://doi.org/10.1016/j.palaeo.2010.09.003>, 2010.
- 625 Zamanian, K., Pustovoytov, K., and Kuzyakov, Y.: Pedogenic carbonates: Forms and formation processes, <https://doi.org/10.1016/j.earscirev.2016.03.003>, 1 June 2016.
- Zhuang, G., Hourigan, J. K., Koch, P. L., Ritts, B. D., and Kent-Corson, M. L.: Isotopic constraints on intensified aridity in Central Asia around 12Ma, *Earth Planet Sci Lett*, 312, 152–163, <https://doi.org/10.1016/j.epsl.2011.10.005>, 2011.